J Mater Sci (2014) 49:1868–1874
DOI 10.1007/s10853-013-7875-7

Double-sided transparent electrodes of TiO_2 nanotube arrays for highly efficient CdS quantum dot-sensitized photoelectrodes

Chong Chen · Fumin Li · Guoqiang Li · Furui Tan · Shengjun Li · Lanyu Ling

Received: 16 August 2013 / Accepted: 8 November 2013 / Published online: 21 November 2013

Abstract A novel double-sided CdS quantum dots-sensitized TiO_2 nanotube (TNT)/ITO photoelectrode is fabricated to improve the energy conversion efficiencies of quantum dots-sensitized solar cells (QDSCs). Our experimental results show that the double-sided CdS quantum dots-sensitized TNT/ITO photoelectrodes show enhanced light absorption. As a consequence, the photoelectrochemical response of the CdS/TNT/ITO photoelectrode is much improved compared with single-sided CdS sensitized TNT arrays on Ti substrate (i.e., CdS/TNT/Ti photoelectrode). An optimum conversion efficiency of 7.5 % is achieved by the double-sided CdS(15)/TNT/ITO photoelectrode, which is an enhancement of about 120 % when compared with the single-sided CdS/TNT/Ti photoelectrode. Our results demonstrate that the energy conversion efficiencies of QDSCs can be improved by designing a new photoelectrode structure.

Introduction

Quantum dot-sensitized solar cells (QDSCs) have attracted a great deal of attention as an alternative to conventional thin film photovoltaic (PV) devices due to the outstanding optoelectronic properties of quantum dots (QDs), their simple fabrication procedure and low cost. The photoelectrodes of QDSCs are typically TiO_2 nanoparticle porous films. In recent years, although QDSCs are progressing very rapidly [1–5], the energy conversion efficiencies of QDSCs still lag behind those of dye-sensitized solar cells. The main reasons for the low efficiencies of QDSCs are low light-harvesting efficiency of QDs, low QDs loading amount due to small surface area in nanoparticle porous photoelectrode, slow electron transport, and the charge recombination at the photoelectrode surface [6]. For increasing the efficiency of QDSCs, considerable efforts have been made to improve the development of more efficient photoelectrode materials, such as highly ordered one-dimensional (1D) TiO_2 nanotube (TNT) photoelectrodes. Compared with TiO_2 nanoparticle porous films, TNT arrays were found to be superior in light-harvesting efficiency and electron transport ability due to its 1D channel [7], in which the internal light scattering was enhanced and the electron transfer through TNT photoelectrodes was promoted. Furthermore, the photogenerated charge recombination at the photoelectrode surface was suppressed by promoting faster electron transport. It has been demonstrated that the QDSCs-based TNT photoelectrodes showed higher energy conversion efficiencies than those of QDSCs-based TiO_2 nanoparticle electrodes [8]. Nevertheless, to further improve the conversion efficiencies of QDSCs based TNT photoelectrodes, there are still some issues to be resolved, such as low QDs loading amount due to the insufficient surface area for QDs and low light-harvesting efficiency.

The TNT arrays can be fabricated by a variety of methods including electrochemical anodization [9–12], hydrothermal synthesis [13], and template-assisted synthesis [14]. For the TNT photoelectrodes in QDSCs, most of the TNT arrays were directly grown on the titanium

C. Chen (✉) · F. Li (✉) · G. Li · F. Tan · S. Li · L. Ling
Henan Key Laboratory of Photovoltaic Materials, Henan University, Kaifeng 475004, People's Republic of China
e-mail: chongchen@henu.edu.cn

F. Li
e-mail: lfm0613@gmail.com

C. Chen · F. Li · G. Li · F. Tan · S. Li · L. Ling
School of Physics and Electronics, Henan University, Kaifeng 475004, People's Republic of China

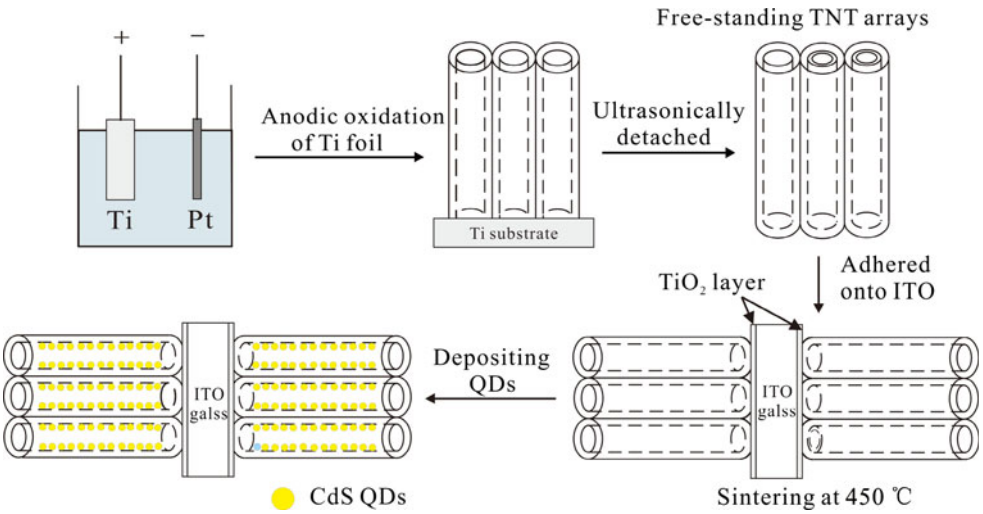

Fig. 1 Scheme for fabricating a double-sided CdS sensitized TNT/ITO photoelectrode

substrate (TNT/Ti) through electrochemical anodization of titanium metal in non-aqueous electrolytes [10–12]. However, only the QDs deposited on the illuminated side of such TNT/Ti-based photoelectrode can contribute to the light absorption due to the opaque Ti substrate, which suggests that the incident light can not be absorbed by the QDs on the other side of TNT/Ti-based photoelectrode and therefore leads to the waste of light absorbing materials (*i.e.*, QDs) and the energy loss of incident light. Here, aiming at these issues, the transparent double-sided CdS QDs-sensitized TNT arrayed photoelectrodes are reported, in which the TNT arrays are oriented perpendicular to the double-sided indium tin oxide (ITO) glass substrates (i.e., double-sided TNT/ITO photoelectrode). Such photoelectrode was first fabricated using a process involving flaking the anodic TNT-array film off the Ti substrate and adhering it onto double-sided ITO glass by sol–gel processed NP-TiO_2 paste [15] and then sintering at high temperature. Several methods have been used to detach the TNT films from the Ti substrate, such as ultrasonication [16, 17], N_2 gas blowing combined with methanol wetting [18], solvent-evaporation [19], solution immersion [20], and two-step anodization [15] methods. In this study, ultrasonication method was selected. Moreover, the detached TNT arrays can also be transferred and adhered onto the single-sided FTO glass using Ti isopropoxide solution as a paste [21]. After the fabrication of double-sided TNT/ITO photoelectrodes, the as-prepared photoelectrodes were sensitized with CdS QDs by chemical-bath deposition (CBD). The detailed synthetic strategy is illustrated in Fig. 1.

In comparison with the commonly used opaque TNT-Ti photoelectrode with single-sided CdS sensitized structure, such fabricated photoelectrode with double-sided CdS sensitized structure provides more space to deposit CdS QDs and more channels to transfer electron to ITO glass substrate, which enhances simultaneously the light absorption and carrier collection of photoelectrodes. To our knowledge, there is no work dedicated to the CdS QDs-sensitized solar cells based on the transparent double-sided TNT/ITO photoelectrode. Only several similar double-sided photoelectrodes, such as double-sided TiO_2/Ti/TiO_2 [22], ZnO/ITO/ZnO [3], and TiO_2/FTO/Cu–Ti–O [23], are designed and fabricated for photoelectrochemical hydrogen generation. Therefore, our study demonstrates an innovative approach for improving the photoelectrode structure for highly efficient QDSCs.

Experiment section

Materials

ITO (≤15 Ω/□, Wuhu Token Sci. Co., Ltd., China) sheet glass, Titanium foil (Ti, Sigma-Aldrich, 0.25 mm thickness, 99.7 % purity), cadmium chloride ($CdCl_2$, Kanto Chemical Co., 98.0 %), ammonium fluoride (NH_4F, Sigma-Aldrich, 98+ %), sodium sulfide nonahydrate (Na_2S, Sigma-Aldrich, 98.0 %), $Ti(OCH_2CH_2CH_2CH_3)_4$ ($Ti(OBu)_4$, Sigma-Aldrich, 97 %), and ethylene glycol (Junsei Chemical Co., 99.0 %) are used as received.

Synthesis of double-sided TNTs arrays/ITO and TNTs/Ti films

Titanium foils were sonicated successively in acetone, ethanol and deionized (DI) water for 10 min respectively, and dried in air. The growth of TNT arrays was accomplished by direct anodization of the as-prepared Ti foil in a two electrode electrochemical cell with a platinum foil as the counter electrode at 55 V for 16 h at room temperature, which contained 0.25 wt% NH_4F and 0.75 wt% DI water in ethylene glycol (99.0 wt%). The experimental procedure is similar to our previous papers [10, 24]. The anodized samples were washed successively in ethanol and DI water to remove the occluded ions and dried in a N_2 stream. After that, the dried

samples were ultrasonicated with DI water until the Ti nanotube-array films were detached from the Ti substrate. Then, the Ti nanotube-array films were adhered onto both sides of ITO glass with a drop of TiO_2 sol containing $Ti(OBu)_4$ and polyethylene glycol and then annealed at 450 °C for 1 h in air to form crystalline anatase TiO_2 phase, which is similar to that described by Kuang et al. [25]. After annealing, the as-prepared TNT-array films on double-sided ITO glass substrates (i.e., double-sided TNT/ITO films) were naturally cooled down to room temperature in air. For comparison, the TNT-arrays on Ti substrates (i.e., TNT/Ti films) for the single-sided opaque CdS(n)/TNT/Ti electrodes were also fabricated by the same process.

Synthesis of doubled-sided CdS/TNT/ITO and CdS/TNT/Ti electrodes

Doubled-sided CdS-sensitized TNT/ITO and CdS/TNT/Ti electrodes were synthesized by sequential CBD, as described in our previous papers [10, 24]. Typically, one CBD process was performed at room temperature by dipping the crystallized doubled-sided TNT/ITO electrodes in a 0.05 M Na_2S aqueous solution for 1 min, rinsing it with DI water, and then dipped in a 0.05 M $CdCl_2$ aqueous solution for 1 min, followed by washing it again with DI water. The doubled-sided CdS-sensitized TNT/ITO and CdS/TNT/Ti electrodes after n cycles of CdS deposition were denoted as CdS(n)/TNT/ITO and CdS(n)/TNT/Ti, respectively. In this study, the cycle number $n = 5$, 10, 15, and 20.

Characterization

The surface morphology and structure of the as-prepared electrodes were characterized using a scanning electron microscope (SEM) (JSM-7001F, Japan Electron Optics Laboratory Co., Ltd., Tokyo, Japan) and power X-ray diffractometry (XRD) (DX-2500; Dandong Fangyuan Instrument Co., Ltd., Dandong, China), respectively. The UV–Vis absorbance spectroscopy was obtained from a UV–Vis spectrophotometer (UV-2550, Shimadzu Corporation, Kyoto, Japan). The current–voltage characteristics of as-prepared samples were measured in a 250-mL quartz cell with an electrochemical workstation (CHI660E, Shanghai Chenhua Instruments Co., Ltd., Shanghai, China) using a three-electrode configuration with the as-prepared samples as working electrode, a Pt foil counter electrode and a saturated Ag/AgCl reference electrode under simulated AM 1.5G illumination (100 mW cm^{-2}) provided by a solar simulator equipped with a 500 W Xe lamp. The electrolyte was 1.0 M Na_2S aqueous solution. The photocurrent responses of the working electrodes with a surface area of 0.04 cm^{-2} were recorded during a voltage sweep from −1.3 to 0 V.

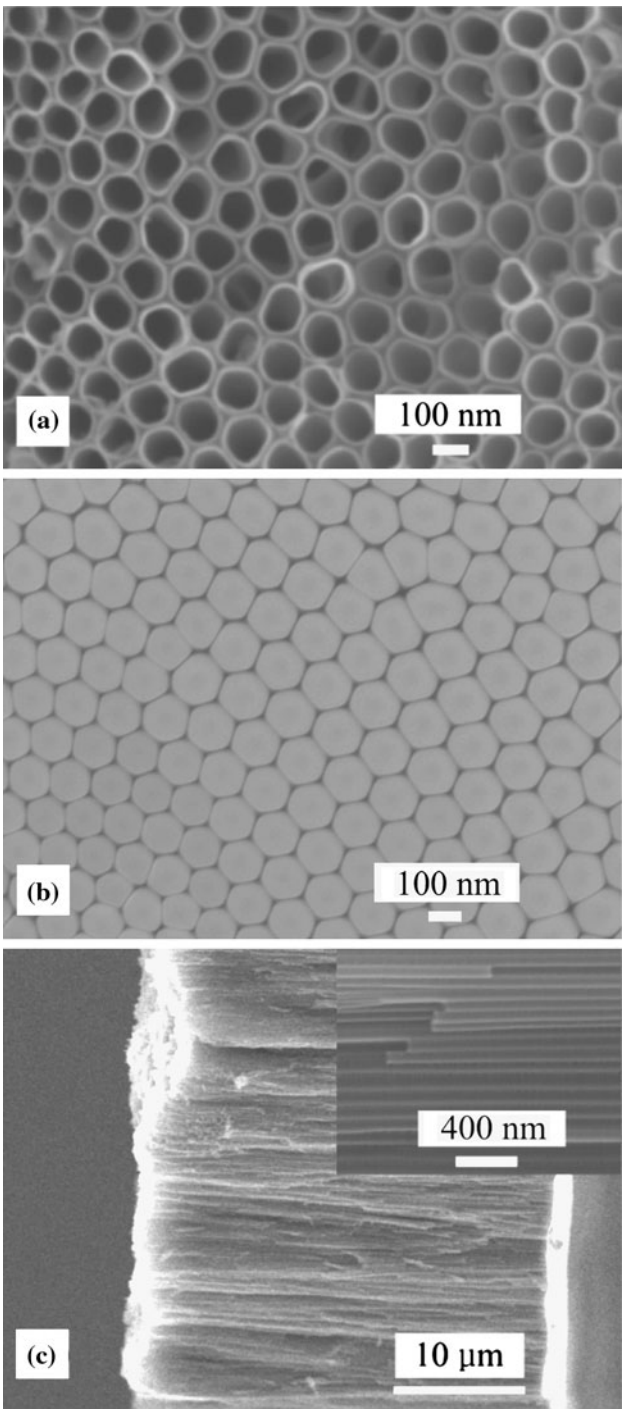

Fig. 2 SEM images showing **a** top view, **b** bottom view, and **c** cross-sectional view of free-standing TiO_2 nanotube arrays

Results and discussion

Figure 2a shows a typical surface SEM image of as-prepared free-standing crystallized TNT membrane, which shows that the TNT arrays still retain a regularly arranged pore structure after they are detached from the Ti substrate. The average diameter of the TNTs is about 142 nm and the

thickness of the wall of the TNTs is about 12 nm. Figure 2b shows the bottom view of the free-standing TNT membrane. It can be seen that the TNTs were packed in approximately hexagonal symmetry. Figure 2c shows the cross-sectional view of the TNT arrays showing that the TNTs of about 26 μm in length are compact and stand vertically.

Figure 3a shows the surface SEM image of the TNT/ITO film covered by CdS QDs after 15 CBD cycles (i.e., CdS(15)/TNT/ITO film). For a comparison, the surface SEM image of the CdS(10)/TNT/ITO film is shown in the inset to Fig. 3a. It can be found after 10 cycles of CBD process, individual CdS QDs with average diameters of ~8 nm have been assembled uniformly onto the TNTs and the aggregation of CdS QDs is not obvious. Besides, the inner diameter of the TNT decreased slightly due to the deposition of CdS QDs on the nanotube wall. Similar phenomenon is also reported by Lin et al. [26]. However, for the CdS(15)/TNT/ITO electrode, it can be found that a large ratio of TNTs is covered by the aggregation of the CdS QDs when the CBD cycle number n increases up to 15 and the size of CdS nanoparticle increases with the cycle number n, which is consistent with the previously reported results [10, 26].

Figure 3b clearly displays the cross-section of the CdS(15)/TNT/ITO film, which shows a structure of three layers: the top layer of CdS-sensitized TNT arrays, the middle layer of TiO_2 film with a thickness of about 1 μm adhered onto ITO glass, and the bottom layer of ITO substrate. The crystallinity of the CdS(15)/TNT/ITO film was characterized by XRD, as shown in Fig. 3c. The diffraction peaks of TiO_2 (marked with T) are clearly observed, corresponding to an anatase TiO_2 (JCPDS 84-1286) [27]. The observed diffraction peaks of CdS (marked with C) can be referred to a hexagonal CdS (1 0 1), (2 2 0), which is in agreement with our previous results [10, 24].

The UV–Vis absorption spectra of the double-sided CdS QDs-sensitized TNT/ITO films, i.e., CdS(n)/TNT/ITO films ($n = 0$, 5, 10, and 15) are shown in Fig. 4a. It can be seen that, the plain double-sided TNT/ITO film absorbs mainly the light with wavelengths smaller than 400 nm, which is similar to the case of TNT film on Ti substrate [26, 28]. After CdS deposition, the absorbance of the spectra of the CdS(n)/TNT/ITO films increase significantly in the UV region as well as the visible region, which is mainly due to the light absorption of deposited CdS QDs. In addition, the absorbance of the spectra of the CdS(n)/TNT/ITO films ($n = 5$ and 10) increase with the cycle number n, which is due to an increased adsorption amount of CdS QDs. For the CdS(15)/TNT/ITO film after 15 CBD cycles, the light absorption property is further improved in the 483–600 nm wavelength region. However, compared to the CdS(10)/TNT/ITO film, the absorbance of the spectra of the CdS(15)/TNT/ITO film in the 350-483 nm wavelength region decreases slightly. For the CdS(10)/$CuInS_2$(2)/TNTs film [10], similar phenomenon has also been observed. This phenomenon is probably due to the quantum size effect. The size of the individual CdS QD will increase with the increasing of cycle number, which might decrease the band gap of CdS QD due to gradually increased CdS particle size.

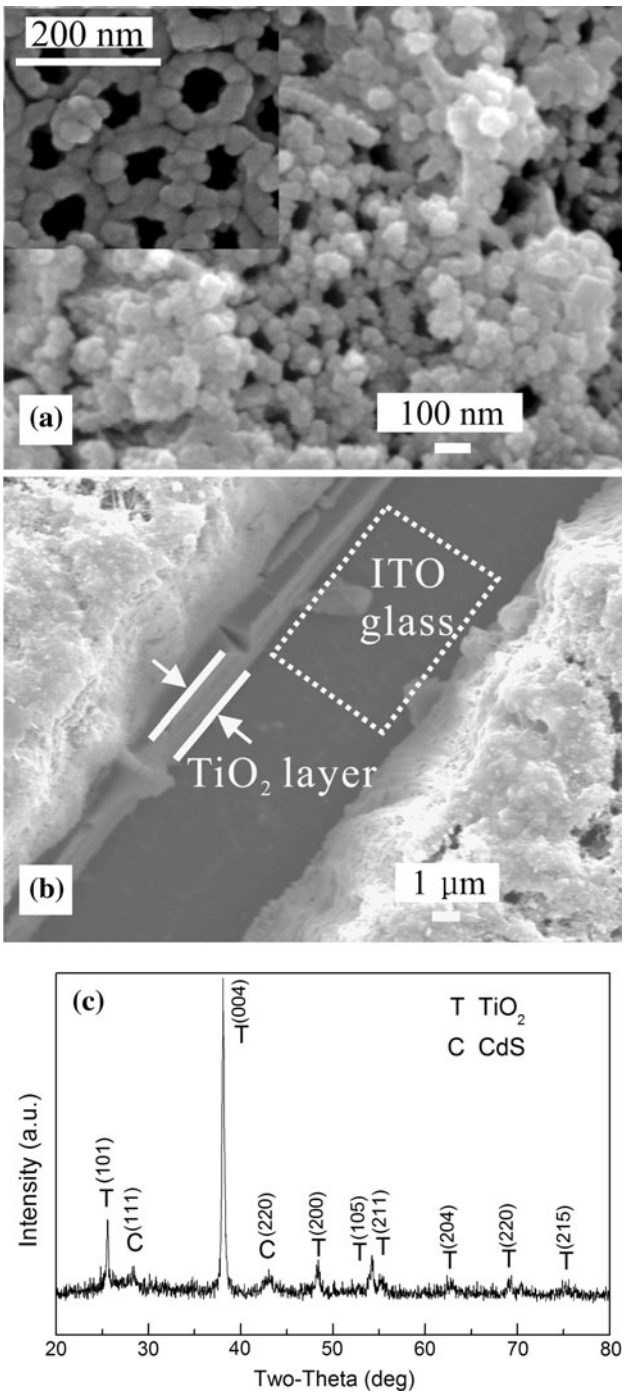

Fig. 3 **a** Top view and **b** cross-sectional SEM images of the CdS(15)/TNT/ITO film. **c** The XRD pattern of the free-standing double-sided CdS(15)/TNT film. The surface SEM image of the CdS(10)/TNT/ITO film is shown in the *inset* to Fig. 3a

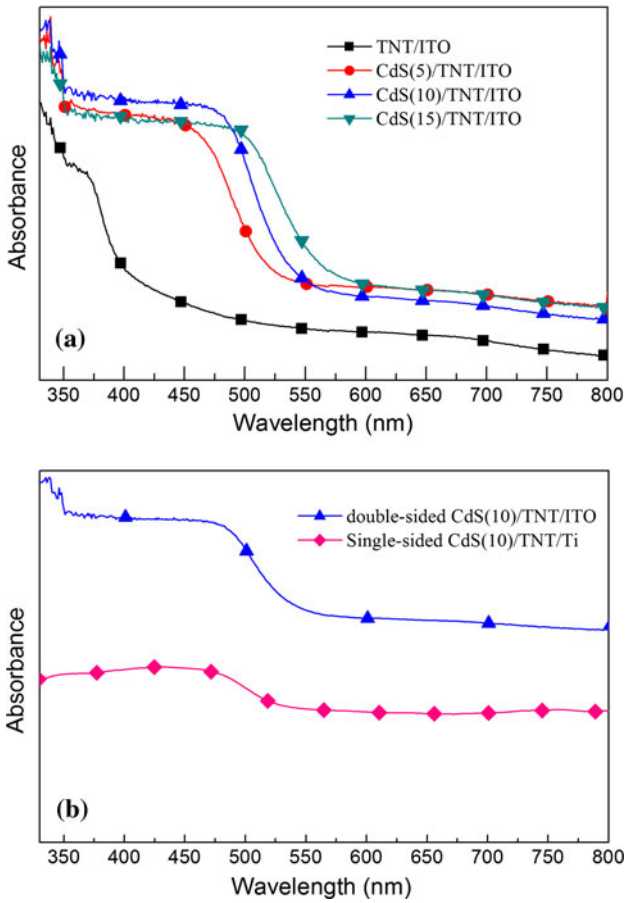

Fig. 4 UV–Vis absorption spectrum of **a** the plain TNT/ITO, double-sided CdS(n)/TNT/ITO films (n = 5, 10, and 15) and **b** the double-sided CdS(10)/TNT/ITO film compare to the single-sided CdS(10)/TNT/IT film

The decreased band gap of the CdS QDs would inevitably lead to a red shit of the absorption of the CdS(15)/TNT/ITO film and result in an increased light absorption in the visible region (<600 nm) and a decreased light absorption in the UV region. It can be clearly seen from Fig. 4a that the spectral photoresponse of the CdS(15)/TNT/ITO film is extended to about 600 nm. In fact, due to the quantum size effect, the significant redshift of the spectral photoresponse can be observed with the increase in the cycle number n not only for the CdS(15)/TNT/ITO film but also for the CdS(n)/TNT/ITO films (n = 5 and 10), as shown in Fig. 4a, which is similar to previously reported results [24, 29]. For example, the spectral photoresponse of the CdS(5)/TNT/ITO, CdS(10)/TNT/ITO films is extended to about 525 and 550 nm, respectively.

In addition, compared to the plain TNT/ITO film, a slight increase in the light absorption of the CdS(n)/TNT/ITO films (n = 5, 10, and 15) films in near-infrared (NIR) region (wavelength >700 nm) is observed in Fig. 4a, which may be probably due to the electron coupling between TiO_2 and CdS heterostructure [30, 31]. After the CdS QDs were deposited on TiO_2 film, a heterojunction is formed between the TiO_2 nanoparticle and CdS quantum dot, which may make the band gap of the TiO_2/CdS composite system different from that of TiO_2 or CdS due to the electron coupling between TiO_2 and CdS heterostructure. When the band gap of the TiO_2/CdS composite system is even smaller than that of bulk CdS, it is possible that the TiO_2/CdS film has a weak absorption in NIR region.

For a comparison, the absorption spectra of the single-sided opaque CdS(n)/TNT/Ti films were also measured and used to compare with that of double-sided CdS(n)/TNT/ITO film. As an example, Fig. 4b shows the absorption spectrum of the CdS(10)/TNT/Ti and CdS(10)/TNT/ITO films. It can be found that the absorption edge of both the as-prepared CdS(10)/TNT/Ti and CdS(10)/TNT/ITO films showed no obvious difference, which appears at about 550 nm. However, the absorbance of the spectra of the double-sided CdS(10)/TNT/ITO film are significantly enhanced compared with the CdS(10)/TNT/Ti film. Apparently, this phenomenon can be attributed to the enhanced light harvesting capability of double-sided CdS-sensitized TNT/ITO films compared with the single-sided CdS-sensitized TNT/Ti film due to an increased amount of CdS nanoparticles, which shows the potential of this doubled-sided structure in improving the current density of the CdS-sensitized TNT photoelectrode due to the increased light absorption.

To study the photoelectrochemical properties of the plain TNT/ITO and double-sided CdS(n)/TNT/ITO photoelectrodes (n = 5, 10, 15, and 20), photoelectrochemical measurements were performed versus a saturated Ag/AgCl electrode under AM 1.5 G (100 m W cm^{-2}) illumination. Figure 5 shows the J–V characteristics of the CdS(n)/TNT/ITO electrodes. It can be observed that the dark current density of the plain TNT/ITO electrode is negligible. Under AM 1.5 G (100 m W cm^{-2}) illumination, all electrodes showed pronounced photoresponse. The saturated photocurrent density of the plain TNT/ITO electrode is about 0.36 mA cm^{-2}, which is comparable with that of the plain TNT/Ti electrode [24]. The open circuit voltage (V_{oc}) of the plain TNT/ITO electrode is about 1.0 V. After the deposition of CdS QDs, the open circuit voltage of the CdS(n)/TNT/ITO photoelectrodes does not change obviously. However, the photocurrent density of the CdS(n)/TNT/ITO photoelectrode is enhanced substantially compared to the plain TNT/ITO photoelectrode, which can be attributed to the improved visible light absorption by the CdS QDs, as shown in Fig. 4a. Moreover, the photocurrent density of the CdS(n)/TNT/ITO photoelectrode increases markedly with the cycles of CdS deposition ($n < 15$), resulting from an higher incorporated amount of CdS that can induce a higher photocurrent density. However, when the cycle number n increases further ($n > 15$), the

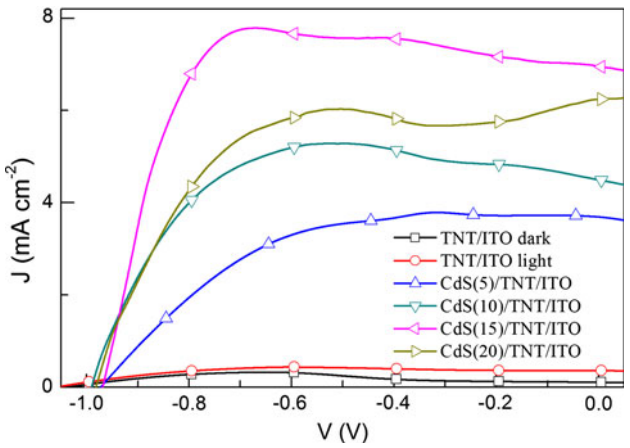

Fig. 5 J–V characteristics of the plain TNT/ITO and double-sided CdS(n)/TNT/ITO photoelectrodes (n = 5, 10, and 15)

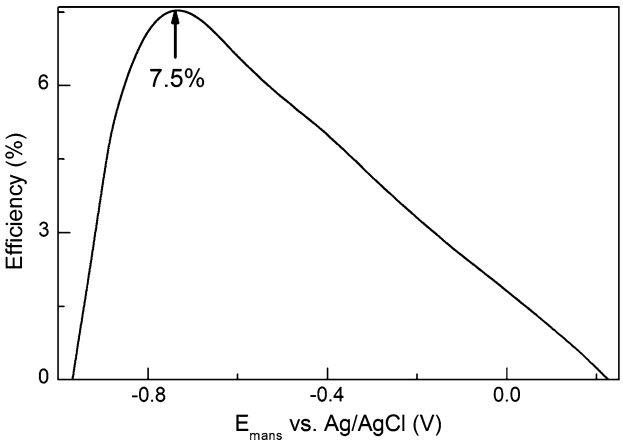

Fig. 6 The photoconversion efficiencies of the double-sided CdS(15)/TNT/ITO electrode

photocurrent density for an applied potential decreases, which may be explained by the fact that the light absorption of CdS QDs in the nanotubes would be less effective due to the aggregation of CdS QDs on the surface of the TNT film. This explanation can be supported by Fig. 3a. A similar result was also observed in previous TNT/Ti-based CdS QDSCs [24, 28]. The highest photocurrent density at short-circuit (J_{sc}) of 6.95 mA cm^{-2} is achieved for the CdS(15)/TNT/ITO photoelectrode, which is much larger than the previously reported value (about 4.8 mA cm^{-2}) of the single-sided opaque TNT/Ti-based CdS QDSCs [24] and the highest J_{sc} of about 6.0 mA cm^{-2} for the double-sided CdS/CdSe QDs-sensitized ZnO nanowire arrays [3].

The photoconversion efficiency η of the double-sided CdS(n)/TNT/ITO photoelectrodes (n = 5, 10, 15, and 20) as a function of applied potential (vs. Ag/AgCl) is calculated as [32] $\eta\ \% = [(\text{total power output} - \text{electric power input})/\text{light power input}] \times 100\ \% = j_p\ [(E_{rev} - |E_{app}|)/I_0] \times 100$, where j_p is the photocurrent density (mA cm^{-2}), E_{rev} (1.23 V/NHE) is the standard state-reversible potential, E_{app} is the applied potential, and I_0 is the power density of incident light (mW cm^{-2}). In addition, E_{app} equals the differences between E_{means} and E_{aoc} (i.e., $E_{app} = E_{means} - E_{aoc}$), where E_{means} is the electrode potential (vs. Ag/AgCl) of the working electrode at which photocurrent was measured under illumination and E_{aoc} is the electrode potential (vs. Ag/AgCl) of the same working electrode under open circuit conditions, under the same illumination and in the same electrolyte. Our calculation result shows that the double-sided CdS(15)/TNT/ITO photoelectrode demonstrates the best PV performance. Only the calculation result for the double-sided CdS(15)/TNT/ITO photoelectrode is shown in Fig. 6 for clarity. It clearly shows that a maximum photoconversion efficiency of about 7.5 % was achieved at an applied potential of −0.73 V versus Ag/AgCl, which is about 120 % higher than the highest efficiency (3.3 %) of the single-sided opaque TNT/Ti-based CdS QDSCs [10] and far higher than that (<2 %) of the QDSCs based on the CdS-sensitized mesoscopic TiO_2 films [33, 34]. The largely enhanced photoconversion efficiency clearly demonstrates the advantage of the transparent TNT/ITO photoelectrodes with double-sided structure compared to the opaque TNT/Ti photoelectrodes with single-sided structure, indicating that the obtained double-sided photoelectrode has potential application in QDSCs and photocatalysis.

Conclusions

In conclusion, double-sided CdS-sensitized TNTs arrayed photoelectrodes were successfully fabricated via ultrasonic treatment of anodized TNT/Ti foil, adhesion of free-standing TNT membrane to the double-sided ITO glass using a drop of a mixture solution of Ti $(OBu)_4$ and polyethylene glycol. In comparison to single-sided opaque TNT/Ti-based electrode, this double-sided sensitized photoelectrode shows enhanced light absorption. Moreover, an optimum conversion efficiency of 7.5 % can be achieved by the double-sided CdS(15)/TNT/ITO photoelectrode, which is about 120 % higher than the highest efficiency of the single-sided CdS/TNT/Ti photoelectrode. The results demonstrate that the photoelectric conversion efficiency of QDSCs can be improved by designing a new photoelectrode structure.

Acknowledgements This work was supported by Henan University distinguished professor startup fund.

References

1. Santra PK, Kamat PV (2012) Mn-doped quantum dot sensitized solar cells: a strategy to boost efficiency over 5%. J Am Chem Soc 134:2508. doi:10.1021/ja211224s

2. Pan ZX, Zhang H, Cheng K, Hou YM, Hua JL, Zhong XH (2012) Highly efficient inverted type-I CdS/CdSe core/shell structure QD-sensitized solar cells. ACS Nano 6:3982. doi:10.1021/Nn300278z
3. Wang GM, Yang XY, Qian F, Zhang JZ, Li Y (2010) Double-sided CdS and CdSe quantum dot co-sensitized ZnO nanowire arrays for photoelectrochemical hydrogen generation. Nano Lett 10:1088. doi:10.1021/Nl100250z
4. Seol M, Kim H, Tak Y, Yong K (2010) Novel nanowire array based highly efficient quantum dot sensitized solar cell. Chem Commun 46:5521. doi:10.1039/C0cc00542h
5. Lee Y-L, Lo Y-S (2009) Highly efficient quantum-dot-sensitized solar cell based on co-sensitization of CdS/CdSe. Adv Funct Mater 19:604. doi:10.1002/adfm.200800940
6. Wang J, Vennerberg D, Lin Z (2011) Quantum dot sensitized solar cells. J Nanoeng Nanomanuf 1:155. doi:10.1166/jnan.2011.1057
7. Zhu K, Neale NR, Miedaner A, Frank AJ (2006) Enhanced charge-collection efficiencies and light scattering in dye-sensitized solar cells using oriented TiO_2 nanotubes arrays. Nano Lett 7:69. doi:10.1021/nl062000o
8. Kongkanand A, Tvrdy K, Takechi K, Kuno M, Kamat PV (2008) Quantum dot solar cells. Tuning photoresponse through size and shape control of CdSe-TiO_2 architecture. J Am Chem Soc 130:4007. doi:10.1021/ja0782706
9. Kuang D, Brillet J, Chen P et al (2008) Application of highly ordered TiO_2 nanotube arrays in flexible dye-sensitized solar cells. ACS Nano 2:1113. doi:10.1021/nn800174y
10. Chen C, Ali G, Yoo SH, Kum JM, Cho SO (2011) Improved conversion efficiency of CdS quantum dot-sensitized TiO_2 nanotube-arrays using $CuInS_2$ as a co-sensitizer and an energy barrier layer. J Mater Chem 21:16430. doi:10.1039/C1jm13616j
11. Lee W, Kang SH, Min SK, Sung YE, Han SH (2008) Co-sensitization of vertically aligned TiO_2 nanotubes with two different sizes of CdSe quantum dots for broad spectrum. Electrochem Commun 10:1579. doi:10.1016/j.elecom.2008.08.038
12. Gao XF, Li HB, Sun WT, Chen Q, Tang FQ, Peng LM (2009) CdTe quantum dots-sensitized TiO_2 nanotube array photoelectrodes. J Phys Chem C 113:7531. doi:10.1021/Jp810727n
13. Zhou Q, Yuan BL, Xu DX, Fu ML (2012) Synthesis, characterization and photocatalytic performance of CdS/TiO_2 nanotube photocatalyst. Chin J Catal 33:850. doi:10.3724/Sp.J.1088.2012.11214
14. Foong TRB, Shen YD, Hu X, Sellinger A (2010) Template-directed liquid ALD growth of TiO_2 nanotube arrays: properties and potential in photovoltaic devices. Adv Funct Mater 20:1390. doi:10.1002/adfm.200902063
15. Lin CJ, Yu WY, Chien SH (2010) Transparent electrodes of ordered opened-end TiO_2-nanotube arrays for highly efficient dye-sensitized solar cells. J Mater Chem 20:1073. doi:10.1039/B917886d
16. Prakasam HE, Shankar K, Paulose M, Varghese OK, Grimes CA (2007) A new benchmark for TiO_2 nanotube array growth by anodization. J Phys Chem C 111:7235. doi:10.1021/jp070273h
17. Chen QQ, Xu DS, Wu ZY, Liu ZF (2008) Free-standing TiO_2 nanotube arrays made by anodic oxidation and ultrasonic splitting. Nanotechnology 19:365708. doi:10.1088/0957-4484/19/36/365708
18. Ali G, Yoo SH, Kum JM, Kim YN, Cho SO (2011) A novel route to large-scale and robust free-standing TiO_2 nanotube membranes based on N_2 gas blowing combined with methanol wetting. Nanotechnology 22:245602. doi:10.1088/0957-4484/22/24/245602
19. Wang J, Lin Z (2008) Freestanding TiO_2 nanotube arrays with ultrahigh aspect ratio via electrochemical anodization. Chem Mater 20:1257. doi:10.1021/cm7028917
20. Albu SP, Ghicov A, Macak JM, Hahn R, Schmuki P (2007) Self-organized, free-standing TiO_2 nanotube membrane for flow-through photocatalytic applications. Nano Lett 7:1286. doi:10.1021/nl070264k
21. Park JH, Lee TW, Kang MG (2008) Growth, detachment and transfer of highly-ordered TiO_2 nanotube arrays: use in dye-sensitized solar cells. Chem Commun 25:2867. doi:10.1039/B800660a
22. Mohapatra SK, Mahajan VK, Misra M (2007) Double-side illuminated titania nanotubes for high volume hydrogen generation by water splitting. Nanotechnology 18:445705
23. Mor GK, Varghese OK, Wilke RHT et al (2008) p-Type Cu−Ti−O nanotube arrays and their use in self-biased heterojunction photoelectrochemical diodes for hydrogen generation. Nano Lett 8:1906. doi:10.1021/nl080572y
24. Chen C, Xie Y, Ali G, Yoo SH, Cho SO (2011) Improved conversion efficiency of CdS quantum dots-sensitized TiO_2 nanotube array using ZnO energy barrier layer. Nanotechnology 22:015202. doi:10.1088/0957-4484/22/1/015202
25. Lei B-X, Liao J-Y, Zhang R, Wang J, Su C-Y, Kuang D-B (2010) Ordered crystalline TiO_2 nanotube arrays on transparent FTO glass for efficient dye-sensitized solar cells. J Phys Chem C 114:15228. doi:10.1021/jp105780v
26. Lai YK, Lin ZQ, Zheng DJ, Chi LF, Du RG, Lin CJ (2012) CdSe/CdS quantum dots co-sensitized TiO_2 nanotube array photoelectrode for highly efficient solar cells. Electrochim Acta 79:175. doi:10.1016/j.electacta.2012.06.105
27. Chen QW, Xu DS (2009) Large-scale, noncurling, and free-standing crystallized TiO_2 nanotube arrays for dye-sensitized solar cells. J Phys Chem C 113:6310. doi:10.1021/Jp900336e
28. Sun WT, Yu Y, Pan HY, Gao XF, Chen Q, Peng LM (2008) CdS quantum dots sensitized TiO_2 nanotube-array photoelectrodes. J Am Chem Soc 130:1124. doi:10.1021/Ja0777741
29. Banerjee S, Mohapatra SK, Das PP, Misra M (2008) Synthesis of coupled semiconductor by filling 1D TiO_2 nanotubes with CdS. Chem Mater 20:6784. doi:10.1021/Cm802282t
30. Ahmed R, Will G, Bell J, Wang H (2012) Size-dependent photodegradation of CdS particles deposited onto TiO_2 mesoporous films by SILAR method. J Nanopart Res 14:1140. doi:10.1007/s11051-012-1140-x
31. Luo J, Ma L, He T, Ng CF, Wang S, Sun H, Fan HJ (2012) TiO2 rutile–anatase core–shell nanorod and nanotube arrays for photocatalytic applications. J Phys Chem C 116:11956. doi:10.1021/jp3031754
32. Khan SU, Al-Shahry M, Ingler WB (2002) Efficient photochemical water splitting by a chemically modified n-TiO_2. Science 297:2243. doi:10.1126/science.1075035
33. Lin S-C, Lee Y-L, Chang C-H, Shen Y-J, Yang Y-M (2007) Quantum-dot-sensitized solar cells: assembly of CdS-quantum-dots coupling techniques of self-assembled monolayer and chemical bath deposition. Appl Phys Lett 90:143517. doi:10.1063/1.2721373
34. Chang C-H, Lee Y-L (2007) Chemical bath deposition of CdS quantum dots onto mesoscopic TiO_2 films for application in quantum-dot-sensitized solar cells. Appl Phys Lett 91:053503. doi:10.1063/1.2768311